J. Fluid Mech. (1976), *vol.* 73, *part* 4, *pp.* 735–752
Printed in Great Britain

Laminar flow in a curved pipe with varying curvature

By S. MURATA, Y. MIYAKE AND T. INABA
Department of Mechanical Engineering, Osaka University, Japan

(Received 6 January 1975)

The steady laminar motion of fluid through pipes of circular cross-section, the curvature of whose centre-line varies locally, is analysed theoretically. The flow in three kinds of pipes whose centre-lines are specified by

$$\hat{y} = a(1+\kappa^2\hat{x}^2)^{\frac{1}{2}}, \quad \hat{y} = a\tanh\kappa\hat{x} \quad \text{and} \quad \hat{y} = a\sin\kappa\hat{x}$$

are treated as the examples of once-, twice- and periodically-curved pipes, respectively. The analysis is valid for any other two-dimensionally curved pipes, when centre-line curvature is small. At very small Reynolds number, the position of maximum axial velocity shifts towards the inner side of the pipe section; at large Reynolds number, on the contrary, it tends to the outer side, owing to centrifugal force. Furthermore, in the latter case, adaptation of the flow follows the change of mean-flow direction, with a phase lag.

1. Introduction

Engineering practice requires extensive knowledge of flow in curved pipes; and numerous studies have been made of it. In particular, almost everything is known about laminar flow in a toroidally-curved pipe of circular cross-section. The Dean number plays a principal role as the similarity parameter in characterizing the flow; and the mathematical procedures for sufficiently small Dean number are fundamentally different from those for fairly large Dean number. In the latter case, theory is based on the boundary-layer concept (Adler 1934; Ito 1969). In the former, perturbation calculations on the basis of Poiseuille flow are useful (Dean 1927, 1928). Numerical integration of the governing equations is adequate in the middle region, where neither procedure is applicable (McConalogue & Srivastava 1968; Greenspan 1973).

The present work deals with the problem of laminar flow in pipes, the curvature of whose centre-line varies locally. There exists no theoretical analysis for these despite the fact that non-uniformly curved pipes have as much practical use as toroidal. Among the different existing approaches, our analysis belongs to the category of low Dean number flow analysis, though the Dean number is not the exact similarity parameter in this case.

Three kinds of curved pipes are treated in this work. However, the details will be described only for a periodically-curved pipe, since the line of thought is completely similar for any other type so long as restrictions imposed in the course of analysis are not violated.

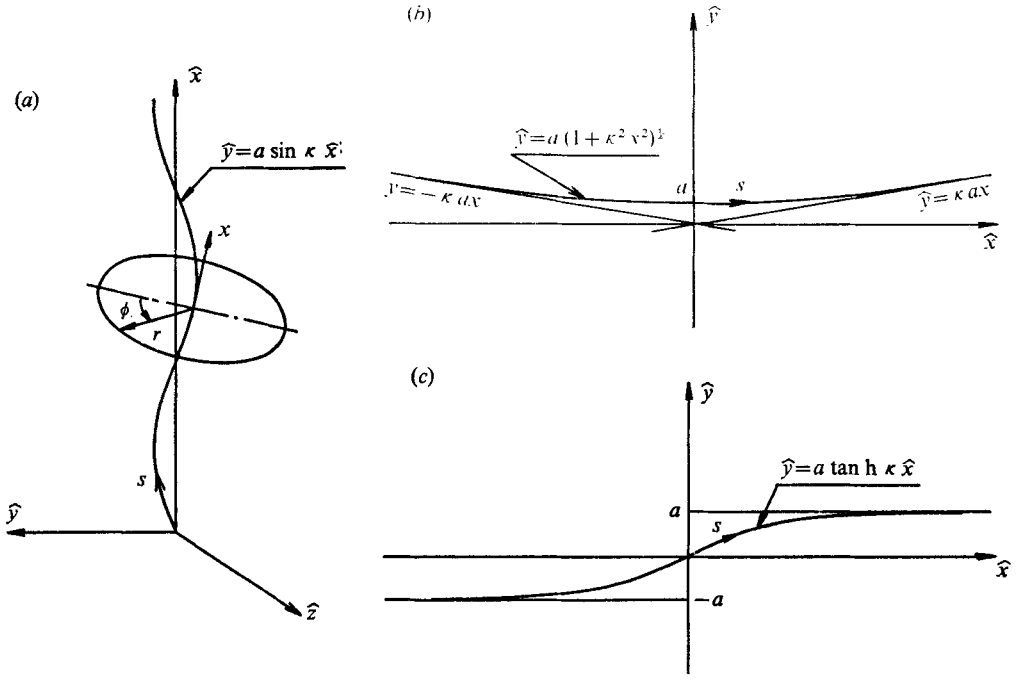

FIGURE 1. Co-ordinate system. (*a*) Periodically-curved pipe. (*b*) Once-curved. (*c*) Twice-curved.

2. Analysis

We consider cases in which the configurations of the centre-line of the curved pipes are specified by two-dimensional curves contained in the $\hat{x}$, $\hat{y}$ plane of a Cartesian co-ordinate system $(\hat{x},\hat{y},z)$. We consider, for instance, the curves

$$\hat{y} = a\sin\kappa\hat{x}, \quad \hat{y} = a(1+\kappa^2\hat{x}^2)^{\frac{1}{2}}, \quad \hat{y} = a\tanh\kappa\hat{x}, \qquad (1)\text{–}(3)$$

in which a and κ are numerical constants. Below we treat these as examples of (i) a periodically curved pipe, (ii) a once-curved pipe, and (iii) a twice-curved pipe. (See figure 1.) In the plane perpendicular to the pipe centre-line, circular co-ordinates (r, ϕ) are defined, and the third co-ordinate axis x is taken in the positive mean-flow direction along the tangent to the pipe centre-line. The co-ordinates (r,ϕ,x) are a right-handed system, and are always orthogonal when the pipe centre-line is a two-dimensional curve. The corresponding velocity components of the flow will be denoted by (u,v,w), respectively. In the following, the velocity v of the fluid is non-dimensionalized by W_0, the maximum velocity in a cross-section of Poiseuille distribution, the static pressure p by ρW_0^2 (density of fluid ρ), and lengths by the pipe radius r_0. The Reynolds number is defined as $Re = W_0 r_0/\nu$, where ν is kinematic viscosity of the fluid.

It is intended to obtain the flow in the region far from the pipe entrance; the influence of the entrance region of the pipe is not taken into account.

The equations of motion and that of continuity are

$$u\frac{\partial u}{\partial r}+\frac{v}{r}\frac{\partial u}{\partial \phi}-\frac{v^2}{r}+\frac{w}{g_{33}^{\frac{1}{2}}}\frac{\partial u}{\partial x}+\Gamma^1_{33}\frac{w^2}{g_{33}}$$
$$=-\frac{\partial p}{\partial r}+\frac{1}{Re}\left[\frac{\partial^2 u}{\partial r^2}+\frac{1}{r}\frac{\partial u}{\partial r}-\frac{u}{r^2}+\frac{1}{r^2}\frac{\partial^2 u}{\partial \phi^2}+\frac{1}{g_{33}}\frac{\partial^2 u}{\partial x^2}-\frac{2}{r^2}\frac{\partial v}{\partial \phi}\right.$$
$$+\frac{\Gamma^1_{33}}{g_{33}}\left(\Gamma^3_{13}u+\Gamma^3_{23}\frac{v}{r}-\frac{\partial u}{\partial r}\right)+\frac{\Gamma^2_{33}}{g_{33}}\left(v-\frac{\partial u}{\partial \phi}\right)$$
$$\left.-\frac{\Gamma^3_{33}}{g_{33}}\frac{\partial u}{\partial x}+\frac{1}{g_{33}}\left\{\frac{w}{g_{33}^{\frac{1}{2}}}\frac{\partial}{\partial x}(\Gamma^1_{33})+2\Gamma^1_{33}\frac{\partial}{\partial x}\left(\frac{w}{g_{33}^{\frac{1}{2}}}\right)\right\}\right], \tag{4}$$

$$u\frac{\partial v}{\partial r}+\frac{v}{r}\frac{\partial v}{\partial \phi}+\frac{uv}{r}+\frac{w}{g_{33}^{\frac{1}{2}}}\frac{\partial v}{\partial x}+\Gamma^2_{33}\frac{rw^2}{g_{33}}$$
$$=-\frac{1}{r}\frac{\partial p}{\partial \phi}+\frac{1}{Re}\left[\frac{\partial^2 v}{\partial r^2}+\frac{1}{r}\frac{\partial v}{\partial r}-\frac{v}{r^2}+\frac{1}{r^2}\frac{\partial^2 v}{\partial \phi^2}+\frac{1}{g_{33}}\frac{\partial^2 v}{\partial x^2}+\frac{2}{r^2}\frac{\partial u}{\partial \phi}\right.$$
$$+\frac{\Gamma^2_{33}}{g_{33}}\left(\Gamma^3_{13}ru-u+\Gamma^3_{23}v-\frac{\partial v}{\partial \phi}\right)-\frac{\Gamma^1_{33}}{g_{33}}\frac{\partial v}{\partial r}-\frac{\Gamma^3_{33}}{g_{33}}\frac{\partial v}{\partial x}$$
$$\left.+\frac{r}{g_{33}}\left\{\frac{w}{g_{33}^{\frac{1}{2}}}\frac{\partial}{\partial x}(\Gamma^2_{33})+2\Gamma^2_{33}\frac{\partial}{\partial x}\left(\frac{w}{g_{33}^{\frac{1}{2}}}\right)\right\}\right], \tag{5}$$

$$u\frac{\partial}{\partial r}\left(\frac{w}{g_{33}^{\frac{1}{2}}}\right)+\frac{v}{r}\frac{\partial}{\partial \phi}\left(\frac{w}{g_{33}^{\frac{1}{2}}}\right)+\frac{w}{g_{33}^{\frac{1}{2}}}\frac{\partial}{\partial x}\left(\frac{w}{g_{33}^{\frac{1}{2}}}\right)+\frac{w}{g_{33}^{\frac{1}{2}}}\left(2\Gamma^3_{31}u+2\Gamma^3_{32}\frac{v}{r}+\Gamma^3_{33}\frac{w}{g_{33}^{\frac{1}{2}}}\right)$$
$$=-\frac{1}{g_{33}}\frac{\partial p}{\partial x}+\frac{1}{Re}\left[\frac{\partial^2}{\partial r^2}\left(\frac{w}{g_{33}^{\frac{1}{2}}}\right)+\frac{1}{r}\frac{\partial}{\partial r}\left(\frac{w}{g_{33}^{\frac{1}{2}}}\right)+\frac{1}{r^2}\frac{\partial^2}{\partial \phi^2}\left(\frac{w}{g_{33}^{\frac{1}{2}}}\right)+\frac{1}{g_{33}}\frac{\partial^2}{\partial x^2}\left(\frac{w}{g_{33}^{\frac{1}{2}}}\right)\right.$$
$$+\frac{w}{g_{33}^{\frac{1}{2}}}\left\{\frac{\partial}{\partial r}(\Gamma^3_{13})+\frac{1}{r^2}\frac{\partial}{\partial \phi}(\Gamma^3_{23})\right\}+\frac{1}{g_{33}}\left\{u\frac{\partial}{\partial x}(\Gamma^3_{13})+\frac{v}{r}\frac{\partial}{\partial x}(\Gamma^3_{23})\right\}$$
$$+\Gamma^3_{13}\left\{\frac{2}{g_{33}}\frac{\partial u}{\partial x}+2\frac{\partial}{\partial r}\left(\frac{w}{g_{33}^{\frac{1}{2}}}\right)+\frac{1}{r}\frac{w}{g_{33}^{\frac{1}{2}}}\right\}+\frac{\Gamma^3_{23}}{r^2}\left\{\frac{2r}{g_{33}}\frac{\partial v}{\partial x}+2\frac{\partial}{\partial \phi}\left(\frac{w}{g_{33}^{\frac{1}{2}}}\right)\right\}$$
$$+\frac{w}{g_{33}^{\frac{1}{2}}}\left\{(\Gamma^3_{12})^2+\left(\frac{\Gamma^3_{33}}{r}\right)^2\right\}-\frac{1}{g_{33}}\left\{\Gamma^1_{33}\frac{\partial}{\partial r}\left(\frac{w}{g_{33}^{\frac{1}{2}}}\right)+\Gamma^2_{33}\frac{\partial}{\partial \phi}\left(\frac{w}{g_{33}^{\frac{1}{2}}}\right)\right.$$
$$\left.\left.-\frac{w}{g_{33}^{\frac{1}{2}}}\frac{\partial}{\partial x}(\Gamma^3_{33})-\Gamma^3_{33}\frac{\partial}{\partial x}\left(\frac{w}{g_{33}^{\frac{1}{2}}}\right)\right\}\right], \tag{6}$$

$$\frac{1}{r}\frac{\partial (ru)}{\partial r}+\frac{1}{r}\frac{\partial v}{\partial \phi}+\frac{\partial}{\partial x}\left(\frac{w}{g_{33}^{\frac{1}{2}}}\right)+\Gamma^3_{31}u+\Gamma^3_{32}\frac{v}{r}+\Gamma^3_{33}\frac{w}{g_{33}^{\frac{1}{2}}}=0. \tag{7}$$

Γ^i_{jk} are the Christoffel symbols of the second kind:

$$\left.\begin{aligned}
&\Gamma^1_{33}=-S\kappa_c g_{33}^{\frac{1}{2}}\cos\phi, \quad \Gamma^2_{33}=\frac{S}{r}\kappa_c g_{33}^{\frac{1}{2}}\sin\phi,\\
&\Gamma^3_{13}=\Gamma^3_{31}=\frac{S}{g_{33}^{\frac{1}{2}}}\kappa_c\cos\phi, \quad \Gamma^3_{23}=\Gamma^3_{32}=-\frac{S}{g_{33}^{\frac{1}{2}}}\kappa_c r\sin\phi,\\
&\Gamma^3_{33}=\frac{1}{g_{33}^{\frac{1}{2}}}\frac{\partial}{\partial x}g_{33}^{\frac{1}{2}}, \quad \text{where} \quad S^2=1+\left(\frac{dy}{dx}\right)^2,
\end{aligned}\right\} \tag{8}$$

for the periodically- (equation (1)) and the twice-curved pipe (equation (3)). For the once-curved pipe (equation (2)), Γ^i_{jk} are the same with opposite sign, except for Γ^3_{33}, which is just as above. The quantity g_{33} is different for each kind of pipe, and is given below in the sections dealing with them. κ_c in (8) is the curvature of the pipe centre-line.

2.1. *Periodically-curved pipe*

We begin with laminar flow in a sinusoidally-curved pipe. Attached orthogonal co-ordinates are related to the rectilinear as follows:

$$\hat{x} = x - \kappa a r \cos\phi \cos\kappa x/S, \quad \hat{y} = a\sin\kappa x + r\cos\phi/S, \quad \hat{z} = r\sin\phi, \tag{9}$$

with $$S = (1+\kappa^2 a^2 \cos^2\kappa x)^{\frac{1}{2}}.$$

This yields $$g_{33}^{\frac{1}{2}} = S(1+\kappa_c r\cos\phi). \tag{10}$$

Putting $r = 0$, (10) reduces to the relation for the pipe centre-line

$$y = a\sin\kappa x, \tag{11}$$

from which is obtained

$$\kappa_c = \kappa^2 a \sin\kappa x/S^3. \tag{12}$$

Here y represents the $\hat{y}$ co-ordinate of pipe centre-line.

Now we consider the case of a pipe with small curvature in the manner usual in treatises on curved pipes. A regular perturbation technique is applied, to get an approximate solution, assuming that the non-dimensional amplitude a of the wavy curve of the pipe centre-line is small. $\mathbf{v}$ and $\mathbf{v}_i$, with components (u, v, w) and (u_i, v_i, w_i), respectively, and p are expanded in a series in a:

$$\mathbf{v} = \mathbf{v}_0 + a\mathbf{v}_1 + a^2\mathbf{v}_2 + \ldots, \quad p = p_0 + ap_1 + a^2 p_2 + \ldots. \tag{13}$$

Then they are substituted in (4)–(7), in which Γ^i_{jk} and g_{33} are also expanded, roughly as above.

The zero-order flow (i.e. that determined by terms of order a^0) becomes Poiseuille. So

$$u_0 = v_0 = 0, \quad w_0 = 1-r^2, \quad p_0 = P_0 - 4x/Re, \tag{14}$$

where P_0 is a constant.

The momentum and continuity equations for the first-order flow are

$$w_0\frac{\partial u_1}{\partial x} - \kappa^2\sin\kappa x\cos\phi w_0^2 = -\frac{\partial p_1}{\partial r} + \frac{1}{Re}\left[\frac{\partial^2 u_1}{\partial r^2} + \frac{1}{r}\frac{\partial u_1}{\partial r} - \frac{u_1}{r^2} + \frac{1}{r^2}\frac{\partial^2 u_1}{\partial\phi^2} + \frac{\partial^2 u_1}{\partial x^2} - \frac{2}{r^2}\frac{\partial v_1}{\partial\phi} - \kappa^3\cos\kappa x\cos\phi w_0\right], \tag{15}$$

$$w_0\frac{\partial v_1}{\partial x} + \kappa^2\sin\kappa x\sin\phi w_0^2 = -\frac{1}{r}\frac{\partial p_1}{\partial\phi} + \frac{1}{Re}\left[\frac{\partial^2 v_1}{\partial r^2} + \frac{1}{r}\frac{\partial v_1}{\partial r} - \frac{v_1}{r^2} + \frac{1}{r^2}\frac{\partial^2 v_1}{\partial\phi^2} + \frac{\partial^2 v_1}{\partial x^2} + \frac{2}{r^2}\frac{\partial u_1}{\partial\phi} + \kappa^3\cos\kappa x\sin\phi w_0\right], \tag{16}$$

$$u_1\frac{\partial w_0}{\partial r} + w_0\frac{\partial w_1}{\partial x} = -\frac{\partial p_1}{\partial x} + \frac{1}{Re}\left[\frac{\partial^2 w_1}{\partial r^2} + \frac{1}{r}\frac{\partial w_1}{\partial r} + \frac{1}{r^2}\frac{\partial^2 w_1}{\partial\phi^2} + \frac{\partial^2 w_1}{\partial x^2} - 6\kappa^2 r\sin\kappa x\cos\phi\right], \tag{17}$$

$$\frac{1}{r}\frac{\partial(ru_1)}{\partial r} + \frac{1}{r}\frac{\partial v_1}{\partial\phi} + \frac{\partial w_1}{\partial x} = 0, \tag{18}$$

with the boundary conditions

$$u_1 = v_1 = w_1 = 0 \quad \text{at} \quad r = 1. \tag{19}$$

The method of separation of variables reduces the partial differential equations (15)–(18) to ordinary ones, the solution of which for arbitrary κ necessitates numerical integration. The behaviour of the solution when $\kappa \ll 1$ can be examined by assuming a solution of the form

$$\mathbf{v}_1 = \kappa^2 \mathbf{v}_{11} + \kappa^3 \mathbf{v}_{12} + \ldots, \quad p_1 = \kappa^2 p_{11} + \kappa^3 p_{12} + \ldots. \tag{20}$$

Substituting these expansions into (16)–(19), and collecting terms of order κ^2, one obtains the governing equations for the flow $(\mathbf{v}_{11}(u_{11}, v_{11}, w_{11}), p_{11})$. The solution for this set is obtained by separation of variables:

$$\left.\begin{aligned}
u_{11} &= -\frac{Re}{288}(1-r^2)^2(4-r^2)\cos\phi\,\frac{1}{\kappa^2 a}\frac{d^2y}{dx^2},\\
v_{11} &= \frac{Re}{288}(1-r^2)(4-23r^2+7r^4)\sin\phi\,\frac{1}{\kappa^2 a}\frac{d^2y}{dx^2},\\
w_{11} &= -r(1-r^2)\left\{\frac{Re^2}{11520}(19-21r^2+9r^4-r^6)-\tfrac{3}{4}\right\}\cos\phi\,\frac{1}{\kappa^2 a}\frac{d^2y}{dx^2},\\
p_{11} &= -\frac{r}{12}(3-6r^2+2r^4)\cos\phi\,\frac{1}{\kappa^2 a}\frac{d^2y}{dx^2}.
\end{aligned}\right\} \tag{21}$$

Here, d^2y/dx^2 is calculated from (11).

In a like manner, the solution of the flow of order κ^3 is obtained:

$$\left.\begin{aligned}
u_{12} &= (1-r^2)^2\left\{\frac{Re^2}{15966720}(3003-3465r^2+1617r^4-231r^6)+\tfrac{1}{6}\right\}\cos\phi\,\frac{1}{\kappa^3 a}\frac{d^3y}{dx^3},\\
v_{12} &= -(1-r^2)\left\{\frac{Re^2}{15966720}(3003-51744r^2+61446r^4-28644r^6\right.\\
&\qquad\left.+3927r^8)+\tfrac{1}{12}(2-r^2)\right\}\sin\phi\,\frac{1}{\kappa^3 a}\frac{d^3y}{dx^3},\\
w_{12} &= \frac{Re}{576}r(1-r^2)\left\{\frac{Re^2}{554400}(32659-48191r^2+35739r^4-14311r^6\right.\\
&\qquad\left.+3014r^8-220r^{10})-(7-5r^2+3r^4)\right\}\cos\phi\,\frac{1}{\kappa^3 a}\frac{d^3y}{dx^3},\\
p_{12} &= \left\{\frac{Re}{15966720}r(93324-11088r^2+83160r^4-27720r^6+2772r^8)\right.\\
&\qquad\left.-\frac{1}{6Re}(1-3r^2)\right\}\cos\phi\,\frac{1}{\kappa^3 a}\frac{d^3y}{dx^3}.
\end{aligned}\right\} \tag{22}$$

The flow of order κ^3 represents the delay of adaptation of the flow to the ever-varying tangential direction of the pipe centre-line, as will be shown later. The streamlines of the secondary flow in a cross-section may be calculated by integrating

$$dr/u_1 = r\,d\phi/v_1. \tag{23}$$

However, these do not always coincide with equi-flow-rate lines, within the order considered.

The above-mentioned solution for small κ is valid in the region $\kappa Re < 1$. We proceed to consider the solution for arbitrary κ, retaining the form of solution in (13). The set of equations (15)–(19) is expected to have a solution of the form

$$\left.\begin{aligned} \psi &= \{F_1(r)\sin\kappa x + F_2(r)\cos\kappa x\}\sin\phi, \\ w_1 &= \{G_1(r)\sin\kappa x + G_2(r)\cos\kappa x\}\cos\phi, \\ u_1 &= \frac{1}{r}\frac{\partial\psi}{\partial\phi}, \\ v_1 &= -\frac{\partial\psi}{\partial r} - \kappa r\,(G_1\cos\kappa x - G_2\sin\kappa x)\sin\phi. \end{aligned}\right\} \tag{24}$$

The stream function ψ satisfies the continuity equation (18), and (15)–(18) are reduced to the following set of ordinary differential equations in the unknown functions $F_1(r)$, $F_2(r)$, $G_1(r)$ and $G_2(r)$, introduced in (24):

$$\begin{aligned} \kappa r\left[F_1''' + \frac{F_1''}{r} - \left(\frac{2}{r^2}+\kappa^2\right)F_1' + \frac{2}{r^3}F_1\right] - \left[(1+\kappa^2r^2)\,G_2'' + (1+3\kappa^2r^2)\frac{G_2'}{r}\right. \\ \left. - (1+2\kappa^2r^2+\kappa^4r^4)\frac{G_2}{r^2}\right] + Re\,[\kappa^2r(1-r^2)\,F_2' - 2F_2 + \kappa(1-r^2)\,(1+\kappa^2r^2)\,G_1 \\ + \kappa^3r(1-r^2)^2] = 0, \end{aligned} \tag{25}$$

$$\begin{aligned} \kappa r\left[F_2''' + \frac{F_2''}{r} - \left(\frac{2}{r^2}+\kappa^2\right)F_2' + \frac{2}{r^3}F_2\right] + \left[(1+\kappa^2r^2)\,G_1'' + (1+3\kappa^2r^2)\frac{G_1'}{r}\right. \\ \left. - 1(1+2\kappa^2r^2+\kappa^4r^4)\frac{G_1}{r^2}\right] - Re\,[\kappa^2r(1-r^2)\,F_1' - 2F_1 - \kappa(1-r^2)\,(1+\kappa^2r^2)\,G_2] \\ - \kappa^2r\{6+\kappa^2(1-r^2)\} = 0, \end{aligned} \tag{26}$$

$$\begin{aligned} G_1''' + \frac{G_1''}{r} - \left(\frac{2}{r^2}+\kappa^2\right)G_1' + \frac{2}{r}\left(\frac{1}{r^2}+\kappa^2\right)G_1 + \frac{\kappa}{r}\left[F_2'' + \frac{F_2'}{r} - \left(\frac{1}{r^2}+\kappa^2\right)F_2\right] \\ + Re\left[2F_1' - \kappa^2(1-r^2)\frac{F_1}{r} + \kappa(1-r^2)\,G_2' - 2\kappa rG_2\right] - \kappa^2\{6+\kappa^2(1-r^2)\} = 0, \end{aligned} \tag{27}$$

$$\begin{aligned} G_2''' + \frac{G_2''}{r} - \left(\frac{2}{r^2}+\kappa^2\right)G_2' + \frac{2}{r}\left(\frac{1}{r^2}+\kappa^2\right)G_2 - \frac{\kappa}{r}\left[F_1'' + \frac{F_1'}{r} - \left(\frac{1}{r^2}+\kappa^2\right)F_1\right] \\ + Re\left[2F_2' - \kappa^2(1-r^2)\frac{F_2}{r} - \kappa(1-r^2)\,G_1 + 2\kappa rG_1 - \kappa^3(1-r^2)^2\right] = 0. \end{aligned} \tag{28}$$

The boundary conditions corresponding to (19) are

$$F_1 = F_1' = 0, \quad F_2 = F_2' = 0, \quad G_1 = G_2 = 0 \quad \text{at} \quad r = 1. \tag{29}$$

Numerical integration of (25)–(28) by means of the Runge–Kutta method is carried out starting from $r = 0$, where F_i and $G_i\,(i = 1, 2)$ are expanded as

$$F_i = a_{i1}r + a_{i3}r^3 + \ldots, \quad G_i = b_{i1}r + b_{i3}r^3 + \ldots. \tag{30}$$

The unknowns are six numerical coefficients a_{i1}, a_{i3} and $b_{i1}\,(i = 1, 2)$, all the other coefficients being related to these. The adequate combination of six unknowns must be determined, so that F_i and G_i satisfy the condition at the goal or at $r = 1$.

Now the flow to order a^1 is completely described. The effect of centre-line curvature upon hydraulic loss does not manifest itself, as is evident from (21) and (22). For this, one is obliged to study the flow of order a^2. Looking for a solution in the range $a \ll 1$, $\kappa \ll 1$, one makes the same sort of manipulations as above, though lengthy, and obtains the governing equations for $(\mathbf{v}_2(u_2, v_2, w_2), p_2)$:

$$\kappa^4\left[u_{11}\frac{\partial u_{11}}{\partial r}+\frac{v_{11}}{r}\frac{\partial u_{11}}{\partial \phi}-\frac{v_{11}^2}{r}+\sin\kappa x\cos\phi w_0(\sin\kappa x\cos\phi r w_0-2w_{11})\right]$$
$$=-\frac{\partial p_2}{\partial r}+\frac{1}{Re}\left[\frac{\partial^2 u_2}{\partial r^2}+\frac{1}{r}\frac{\partial u_2}{\partial r}-\frac{u_2}{r^2}+\frac{1}{r^2}\frac{\partial^2 u_2}{\partial \phi^2}-\frac{2}{r^2}\frac{\partial v_2}{\partial \phi}\right.$$
$$\left.+\kappa^4\sin\kappa x\left\{\cos\phi\frac{\partial u_{11}}{\partial r}-\sin\phi\left(\frac{1}{r}\frac{\partial u_{11}}{\partial \phi}-\frac{v_{11}}{r}\right)\right\}\right], \tag{31}$$

$$\kappa^4\left[u_{11}\frac{\partial v_{11}}{\partial r}+\frac{v_{11}}{r}\frac{\partial v_{11}}{\partial \phi}+\frac{u_{11}v_{11}}{r}-\sin\kappa x\sin\phi w_0(\sin\kappa x\cos\phi r w_0-2w_{11})\right]$$
$$=-\frac{1}{r}\frac{\partial p_2}{\partial \phi}+\frac{1}{Re}\left[\frac{\partial^2 v_2}{\partial r^2}+\frac{1}{r}\frac{\partial v_2}{r^2}-\frac{v_2}{r^2}+\frac{1}{r^2}\frac{\partial^2 v_2}{\partial \phi^2}+\frac{2}{r^2}\frac{\partial u_2}{\partial \phi}\right.$$
$$\left.+\kappa^4\sin\kappa x\left\{\cos\phi\frac{\partial v_{11}}{\partial r}-\sin\phi\left(\frac{1}{r}\frac{\partial v_{11}}{\partial \phi}+\frac{u_{11}}{r}\right)\right\}\right], \tag{32}$$

$$\kappa^4\left[u_{11}\frac{\partial w_{11}}{\partial r}+\frac{v_{11}}{r}\frac{\partial w_{11}}{\partial \phi}+\sin\kappa x\left\{\cos\phi r u_{11}\left(\frac{w_0}{r}-\frac{\partial w_0}{\partial r}\right)-\sin\phi v_{11}w_0\right\}\right]+u_2\frac{\partial w_0}{\partial r}$$
$$=-\frac{\partial p_2}{\partial x}-\kappa^2(3\kappa^2r^2\sin^2\kappa x\cos^2\phi-\tfrac{1}{2}\cos^2\kappa x)\frac{\partial p_0}{\partial x}$$
$$+\frac{1}{Re}\left[\frac{\partial^2 w_2}{\partial r^2}+\frac{1}{r}\frac{\partial w_2}{\partial r}+\frac{1}{r^2}\frac{\partial^2 w_2}{\partial \phi^2}-\kappa^4\sin\kappa x\left\{r\cos\phi\left(\frac{\partial^2 w_{11}}{\partial r^2}+\frac{1}{r^2}\frac{\partial^2 w_{11}}{\partial \phi^2}\right)\right.\right.$$
$$\left.\left.+\sin\phi\frac{1}{r}\frac{\partial w_{11}}{\partial \phi}\right\}+\kappa^4\sin^2\kappa x\left\{r^2\cos^2\phi\left(\frac{\partial^2 w_0}{\partial r^2}-\frac{1}{r}\frac{\partial w_0}{\partial r}\right)-w_0\right\}\right], \tag{33}$$

$$\frac{1}{r}\frac{\partial(ru_2)}{\partial r}+\frac{1}{r}\frac{\partial v_2}{\partial \phi}+\kappa^4\sin\kappa x\,(\cos\phi u_{11}-\sin\phi v_{11})=0. \tag{34}$$

Here terms of order higher than κ^4 are neglected. We restrict ourselves to finding the change in flow rate in the curved pipe compared with that in the straight when the pressure loss between two sections measured along the centre-line of the two pipes is equal; other details will not be touched upon. Because

$$dx/ds = 1-\tfrac{1}{2}\kappa^2a^2\cos^2\kappa x,$$

where s is measured along the centre-line, the above-mentioned condition

$$\partial\overline{p}/\partial s = \partial\overline{p}_0/\partial s$$

gives
$$-\partial p_2/\partial x+\tfrac{1}{2}\kappa^2\cos^2\kappa x(\partial p_0/\partial x)=0.$$

Considering that every term in the governing equations for $(\mathbf{v}_2, p_2)$ contains the factor

$$\sin^2\kappa x\sin\phi\cos\phi=\tfrac{1}{2}\sin^2\kappa x\sin 2\phi,$$

a solution of the form

$$\left.\begin{aligned} u_2 &= \{I_1(r)\cos 2\phi + J(r)\}\kappa^4 \sin^2\kappa x, \\ v_2 &= I_2(r)\sin 2\phi \kappa^4 \sin^2\kappa x, \\ w_2 &= \{H_1(r)\cos 2\phi + H_2(r)\}\kappa^4 \sin^2\kappa x \end{aligned}\right\} \tag{35}$$

is found to be possible. Of the five unknown functions in (35), only $H_2(r)$ is concerned with the mean flow rate. It is easily verified that $J(r)$ is given by

$$J(r) = -Re/576r(1-r^2)^2(4-r^2),$$

from (31). This is then substituted into u_2 in (33), and finally yields

$$\begin{aligned} H_2(r) = \frac{\kappa^4}{32\times 144^2}\Big[& Re^4\left(-\frac{12357}{67200}+\frac{19}{20}r^2-\frac{331}{160}r^4+\frac{99}{40}r^6-\frac{569}{320}r^8\right. \\ & \left.+\frac{157}{200}r^{10}-\frac{33}{160}r^{12}+\frac{1}{35}r^{14}-\frac{1}{640}r^{16}\right) \\ & + Re^2\left(-\frac{2664}{25}+\frac{378}{5}r^2+126r^4-144r^6+54r^8-\frac{126}{25}r^{10}\right) \\ & -\tfrac{1}{64}(3-14r^2+11r^4)\Big]. \end{aligned} \tag{36}$$

The mean flow rate is

$$F_c = 2\pi\int_0^1 r\{(1-r^2)+\tfrac{1}{2}\kappa^4 a^2 H_2(r)\}\,dr = \pi\left[\tfrac{1}{2}+\kappa^4 a^2\int_0^1 rH_2(r)\,dr\right], \tag{37}$$

in non-dimensional form, or, expressed as a ratio to that for a straight pipe $F_s = \frac{1}{2}\pi$, it becomes

$$\frac{F_c}{F_s} = 1-\kappa^4 a^2\left[2\left(\frac{Re^2}{576}\right)^2(0{\cdot}03058)+2\left(\frac{Re}{576}\right)^2(128{\cdot}4)-0{\cdot}010417\right]. \tag{38}$$

2.2. *Once-curved pipe*

The pipe centre-line is assumed to have the configuration

$$y = a(1+\kappa^2 x^2)^{\frac{1}{2}}. \tag{39}$$

Correspondingly, the curvature is

$$\kappa_c = \kappa^2 a/\{(1+\kappa^2 x^2)^{\frac{3}{2}} S^3\}, \quad \text{where} \quad S = \{1+\kappa^4 a^2 x^2/(1+\kappa^2 x^2)\}^{\frac{1}{2}}. \tag{40}$$

The curvilinear co-ordinates (r, ϕ, x) attached to this pipe are related to the rectilinear by

$$\hat{x} = x - \frac{\kappa^2 axr\cos\phi}{(1+\kappa^2 x^2)^{\frac{1}{2}}S}, \quad \hat{y} = a(1+\kappa^2 x^2)^{\frac{1}{2}} + \frac{r\cos\phi}{S}, \quad \hat{z} = r\sin\phi. \tag{41}$$

From (41) we obtain

$$g_{33}^{\frac{1}{2}} = S(1-\kappa_c r\cos\phi). \tag{42}$$

As in § 2.1, a regular perturbation solution with perturbation parameter $\kappa \ll 1$,

$$\mathbf{v} = \mathbf{v}_0 + \kappa^2\mathbf{v}_{*1} + \kappa^3\mathbf{v}_{*2} + \ldots, \quad p = p_0 + \kappa^2 p_{*1} + \kappa^3 p_{*2} + \ldots, \tag{43}$$

is to be looked for. The zero-order solution is, as expected, the Poiseuille flow. A lengthy calculation shows that the governing equations for the first-order flow

(i.e. that of order κ^2) are the same as those for the sinusoidally-curved pipe with modifications $a\mathbf{v}_{11}$ to $\mathbf{v}_{*1}$ and ap_{11} to p_{*1}, respectively, except for the equation of motion for the x component. The discrepancy in this equation of motion is due to the difference in the expansion: i.e. in the present problem the velocity $\mathbf{v}$ is expanded in a single series as

$$\mathbf{v} = \mathbf{v}_0 + \sum_n \kappa^{n+1}\mathbf{v}_{*n},$$

but in the problem discussed in § 2.1 it was expanded in a double series as

$$\mathbf{v} = \mathbf{v}_0 + \sum_m a^m \sum_n n^{n+1}\mathbf{v}_{mn},$$

and it affects only the static pressure. A solution of the above-mentioned system of equations can be obtained just as before. The velocity $\mathbf{v}_{*1}$ is given by (21), with modification of $a\mathbf{v}_{11}$ to $\mathbf{v}_{*1}$. The corresponding static pressure p_{*1} is

$$p_{*1} = -\frac{r}{12}(3-6r^2+2r^4)\cos\phi\,\frac{1}{\kappa^2}\frac{d^2y}{dx^2} - \frac{2a^2}{Re}\left(x - \frac{1}{\kappa}\tan^{-1}\kappa x\right). \tag{44}$$

Flow of order κ^3 is easily shown to be subject to the equations of § 2.1, with replacement of $a\mathbf{v}_{12}$ by $\mathbf{v}_{*2}$ and ap_{12} by p_{*2}. The resulting velocity and pressure are given by (22), with the same replacements. The secondary flow streamlines are calculated by integrating (23) using these velocities.

2.3. *Twice-curved pipe*

The centre-line and its curvature are assumed to be

$$y = a\tanh\kappa x, \quad \kappa_c = 2\kappa^2 a\,\mathrm{sech}^2\kappa x\tanh\kappa x/S^3, \tag{45), (46}$$

respectively, where $S = (1+\kappa^2 a^2\,\mathrm{sech}^4\kappa x)^{\frac{1}{2}}$.

The curvilinear co-ordinates (r,ϕ,x) belonging to this pipe are related to the rectilinear by

$$\hat{x} = x - \kappa a r\cos\phi\,\frac{\mathrm{sech}^2\kappa x}{S}, \quad \hat{y} = a\tanh\kappa x + \frac{r\cos\phi}{S}, \quad \hat{z} = r\sin\phi, \tag{47}$$

and

$$g_{33}^{\frac{1}{2}} = S(1+\kappa_c r\cos\phi). \tag{48}$$

Manipulations are carried out analogous to those of § 2.2. The regular perturbation, with κ assumed to be sufficiently small, yields Poiseuille flow at zero order. The velocity is exactly the same as that in § 2.2, and the static pressure becomes

$$p_{*1} = -\frac{r}{12}(3-6r^2+2r^4)\cos\phi\,\frac{1}{\kappa^2}\frac{d^2y}{dx^2} - \frac{4a^2}{3\kappa\,Re}\tanh\kappa x\,(1+\tfrac{1}{2}\,\mathrm{sech}^2\kappa x). \tag{49}$$

Furthermore, the second-order flow is identical with that in § 2.2.

3. Numerical examples

3.1. *Periodically-curved pipe*

Numerical computations are given below. In them the flow is calculated from (21) and (22) in the range $\kappa Re \ll 1$, and by integrating (25)–(28) for fairly large values of κRe. The results of these two procedures agree well, even when κRe

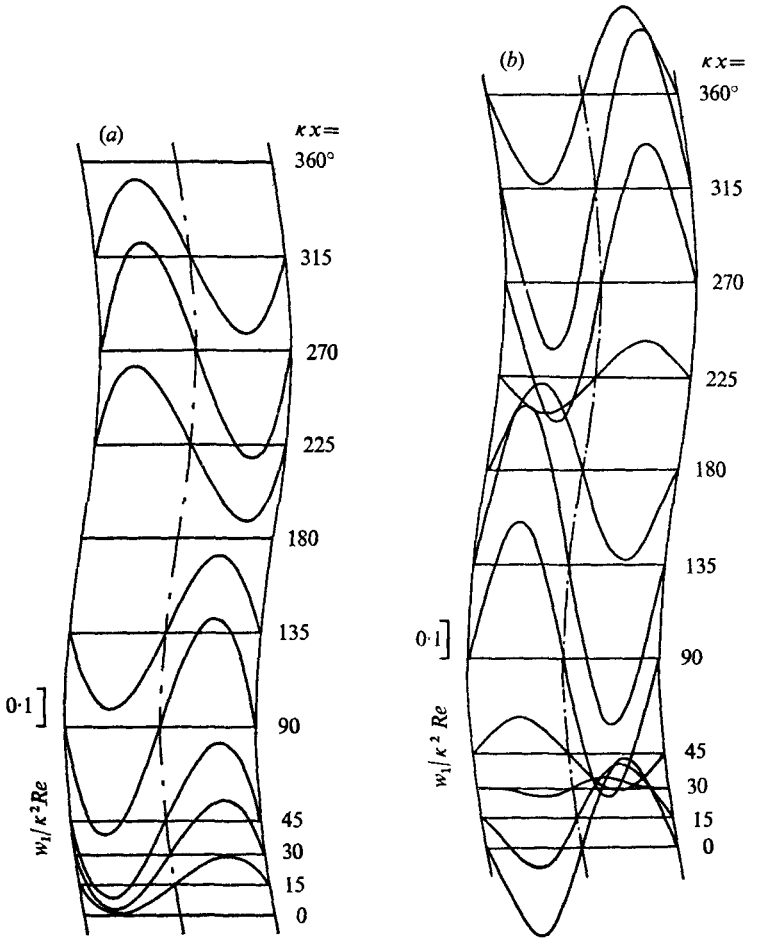

FIGURE 2. Distribution of deviation of axial velocity from that of Poiseuille flow. $\kappa = 0{\cdot}01$, $\sin\phi = 0$. (a) $Re = 1$. (b) $Re = 1000$.

approaches 1. This is to be expected, because $|\mathbf{v}_{11}| \gg |\kappa\mathbf{v}_{12}|$ there, as is evident from (21) and (22).

Figure 2 shows the distribution of deviation of axial velocity from that of Poiseuille flow in succeeding sections of the pipe. Figures 2 (*a*) and (*b*) are respectively for $Re = 1$ and 1000. The pipe waving is exaggerated in the figure, to aid understanding. When the Reynolds number is small, the fluid flows more in the inner part, which is nearer to the centre of the curvature, than in the outer portion of the pipe section. Consequently, the averaged flow path becomes shorter than the length measured along the centre-line. Hence the flow rate becomes larger than in the straight pipe when the same pressure drop between two sections, the same developed distance apart, is assumed. The last term in (38) represents this effect. In the case of a toroidal pipe, with of course constant centre-line curvature, this phenomenon also appears, as pointed out by Larrain & Bonilla (1970). It may be attributed to the general rule that viscous fluid flows so as to

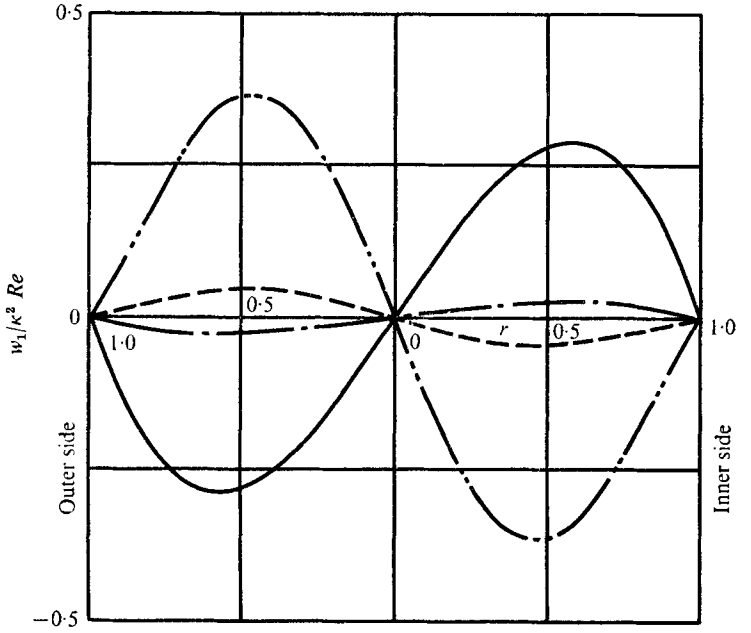

FIGURE 3. Effect of Reynolds number upon the deviation of axial velocity. $\kappa = 0{\cdot}01$, $\kappa x = 90°$, $\sin\phi = 0$. *Re*: ———, 1; — · —, 10; – – – –, 100; — – — –, 1000.

make viscous dissipation minimum if the flow is so slow that inertia terms in the momentum equation are negligible (Ito 1951).

As the Reynolds number increases, the effect of the centrifugal force due to the curving of the pipe becomes pronounced; and at $Re = 1000$ it is the predominant cause of secondary flow (figure 3). Correspondingly, fluid flows more in the outer portion of pipe section then; and, at the same time, the adaptation of the axial flow distribution to the change in curvature of the centre-line is delayed. In figure 2(*b*), at $\kappa x = 0°$, where the curvature vanishes, the axial velocity distribution is still that of upstream sections, where the centrifugal force acts leftwards (in the figure); and, at about $\kappa x = 30°$, w_1 or the deviation from Poiseuille flow due to the pipe curvature vanishes. Furthermore, the maximum w_1 occurs at about $\kappa x = 120$, not 90°, which means that, in this pipe, the effect of curvature appears in the downstream section, delayed by about $\kappa x = 30°$.

Figure 4 shows the variation of flow for different κ, the wavenumber of the sinusoidally-curved pipe centre-line. Figure 4(*a*) is for $Re = 1$. The flow pattern is almost independent of κ when $\kappa \ll 1$; and, as κ increases, the effect of curvature is more and more accentuated in the region nearer the wall, as suggested by the graph for $\kappa = 10{\cdot}0$. Figure 4(*b*) is for $Re = 100$. The delay of adaptation of flow to curvature is more remarkable as the Reynolds number increases; and when $\kappa = 1{\cdot}0$, even at $\kappa x = 90°$, where curvature is maximum, w_1 is larger in the region nearer the inner wall. In this section, the delay of adaptation amounts to about 165°, and the maximum w_1 is at about $\kappa x = 150°$, as is seen in figure 4(*c*).

Figure 5 shows the secondary flow streamlines obtained by integrating (23). The rate of the secondary flow in a section, between two neighbouring streamlines

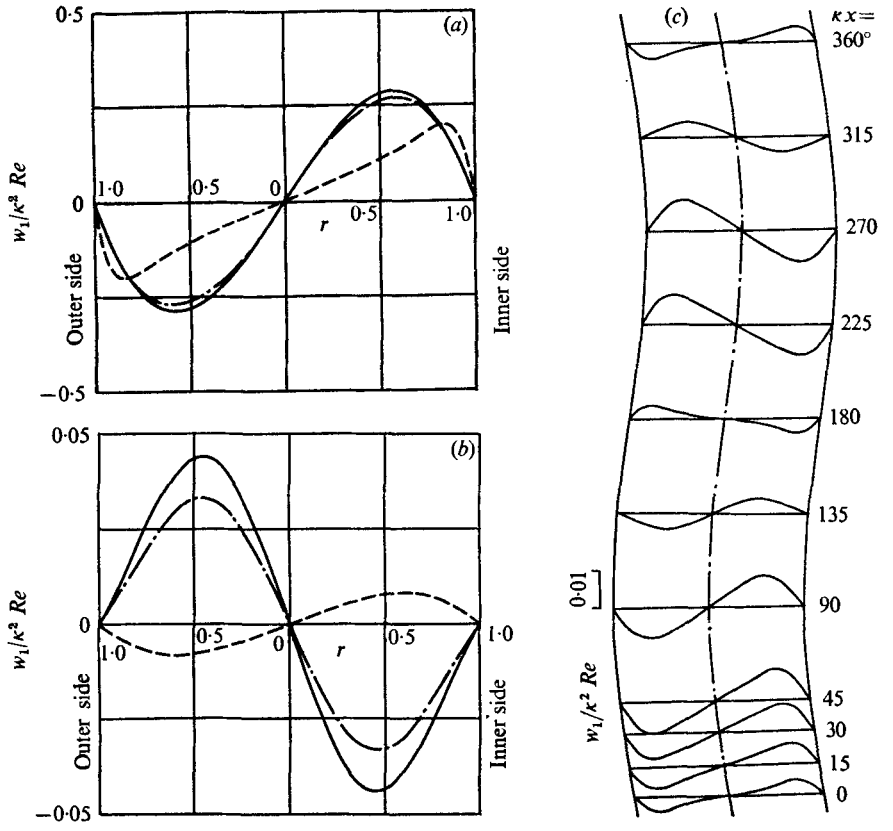

FIGURE 4. Effect of κ upon deviation of axial velocity. $\kappa x = 90°$, $\sin\phi = 0$. (*a*) $Re = 1$. Ordinate is to be read multiplying by a factor 0·1 when $\kappa = 10{\cdot}0$. (*b*) $Re = 100$. (*c*) Distribution of deviation of axial velocity when $Re = 100{\cdot}0$, $\kappa = 1{\cdot}0$.

κ				
	(*a*)	0·1	1·0	10·0
	(*b*)	0·01	0·1	1·0

obtained in this way, cannot be constant along them. The continuity equation (18) shows that the divergence of the secondary flow does not vanish everywhere in the section. Hence, the computed streamlines do not always coincide with equi-flow-rate lines, and only in the section where $\cos\kappa x = 0$ do these lines coincide when the flow to order κ^3 is taken into account. Figure 5(*a*) is the flow in the section $\kappa x = 90°$, and the lines are also the equi-flow-rate lines, which can correspondingly be compared directly with those shown in Dean (1927). Figure 5(*b*) is drawn for the section $\kappa x = 0°$. For both (*a*) and (*b*), the flow rate between two neighbouring streamlines is the same on the line OA.

Figure 6 shows the distribution of circumferential velocity on the line OA of figure 5. Figure 6(*a*) is for various Reynolds numbers; and (*b*) is for various values of κ. When either the Reynolds number or κ is small, the secondary flow is determined locally, and the continuity condition is satisfied two-dimensionally in terms of u and v. In this type of curved pipe, an unusual secondary flow pattern with multi-region or non-circulatory streamlines appears because of non-homogeneity

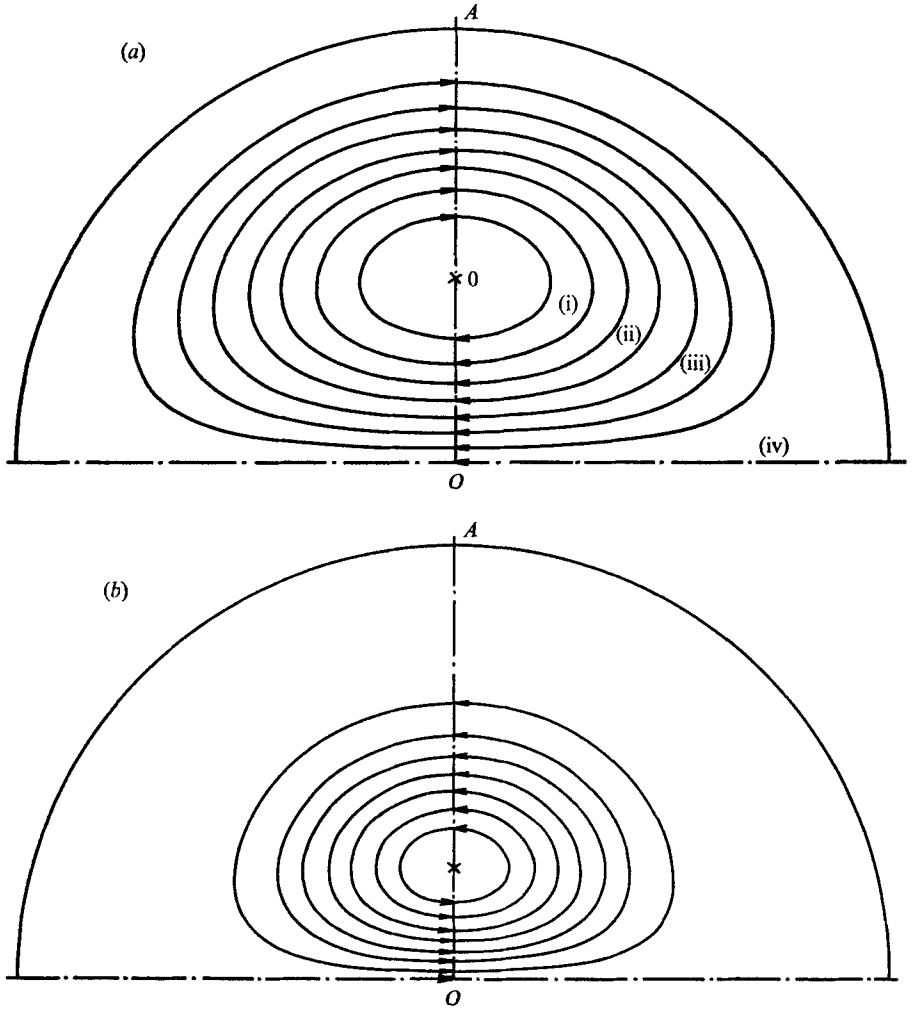

FIGURE 5. Secondary flow streamlines. $Re = 100$, $\kappa = 0{\cdot}01$. (*a*) $\kappa x = 90°$: (i) $q/\kappa^2 a Re = 0{\cdot}0946 \times 10^{-2}$, (ii) 0·1892, (iii) 0·2838, (iv) 0·3784. Also lines of equal flow rate. (*b*) $\kappa x = 0°$.

in speed of adaptation of the secondary flow to curvature. The axial extent of its appearance depends on κ and Re, and is determined by looking for the sections that satisfy

$$v_1 = 0 \quad \text{at} \quad r = 0 \quad \text{and} \quad \partial v_1/\partial r = 0 \quad \text{at} \quad r = 1.$$

This unusual pattern falls in one of two categories depending on κ. When $\kappa \ll 1$, the secondary flow shows no closed streamline. When κ becomes large, the secondary flow streamlines become doubly-centred, and rotate counterwise about one another in an upper/lower half-section.

The typical features of these two cases are shown in figure 7, by means of the v_1 distribution. Figure 7(*a*) is for $\kappa \ll 1$ (i.e. $\kappa = 0{\cdot}01$ and $Re = 1000$). The usual flow pattern is missing in the section between $\kappa x = 7{\cdot}72$ and 10·23°. Figure 7(*b*) is for fairly large κ (i.e. $\kappa = 1{\cdot}0$ and $Re = 100$). The multi-region secondary flow

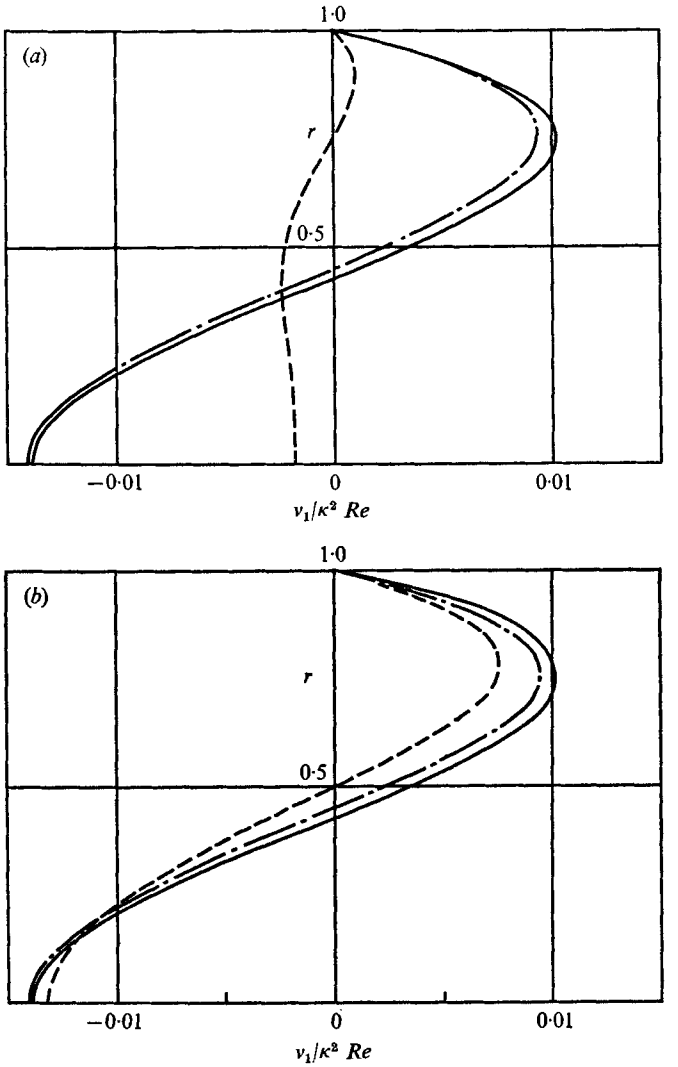

FIGURE 6. Distribution of circumferential velocity. $\kappa x = 90°$, $\phi = 90°$. (*a*) Effects of Re, $\kappa = 0{\cdot}01$. (*b*) Effect of κ, $Re = 100$.

(*a*) Re	$\leqslant 100$	$= 1000$	$= 2000$
(*b*) κ	0·01	0·1	1·0
	———	— — —	- - - - -

appears in the section $\kappa x = 39{\cdot}48$–$75{\cdot}35°$. In this case also, the secondary flow streamlines do not coincide with equi-flow-rate lines. These unusual secondary flow patterns have also been reported for unsteady flow in a toroidal pipe (Lyne 1970), and in a rotating curved pipe (Ito & Motai 1974).

3.2. *Once-curved pipe*

In the case of § 3.1 it is possible to calculate the flow for any value of κ, so long as a is sufficiently small. However, in the present case, the alternative way of

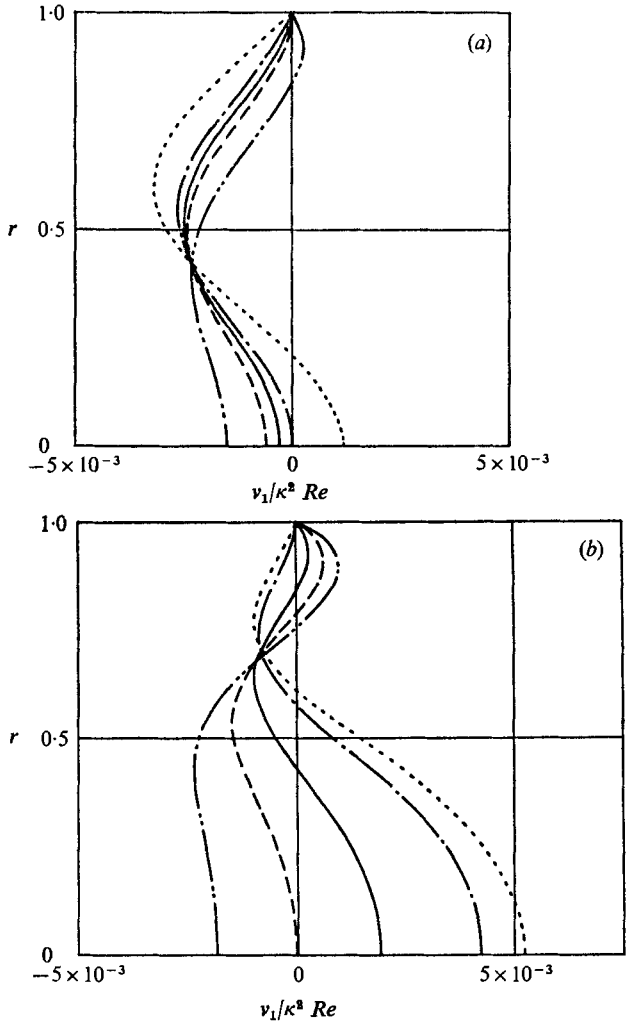

FIGURE 7. Circumferential velocity distribution near the region of inversion of secondary flow direction. (*a*) $\kappa = 0{\cdot}01$, $Re = 1000$. (*b*) $\kappa = 1{\cdot}0$, $Re = 100$.

κx (deg)					
(*a*)	3·0	7·7	9·0	10·2	14·0
(*b*)	30·0	39·5	60·0	75·3	90·0
	·····	— — —	———	- - - -	——— —

obtaining a solution for arbitrary κ by (24)–(30) is impossible, and the solution is severely restricted in the range $\kappa Re \ll 1$. Figure 8 shows the deviation of the axial flow w_s from Poiseuille. Figure 8(*a*) is for $Re = 1$, (*b*) for $Re = 100$. Phenomena analogous to those in a sinusoidally-curved pipe are obtained. The short path is chosen in the curved region when the Reynolds number is small; and increase in the latter makes the effect of the centrifugal force predominant. This results in the positive w_s in the outer part of the pipe section.

The secondary flow streamlines computed by means of (38) coincide with equi-flow-rate lines when $\kappa x = 0$; and are identical with those shown in figure 5(*a*) with the flow direction reversed. The secondary flow streamlines in other sections are

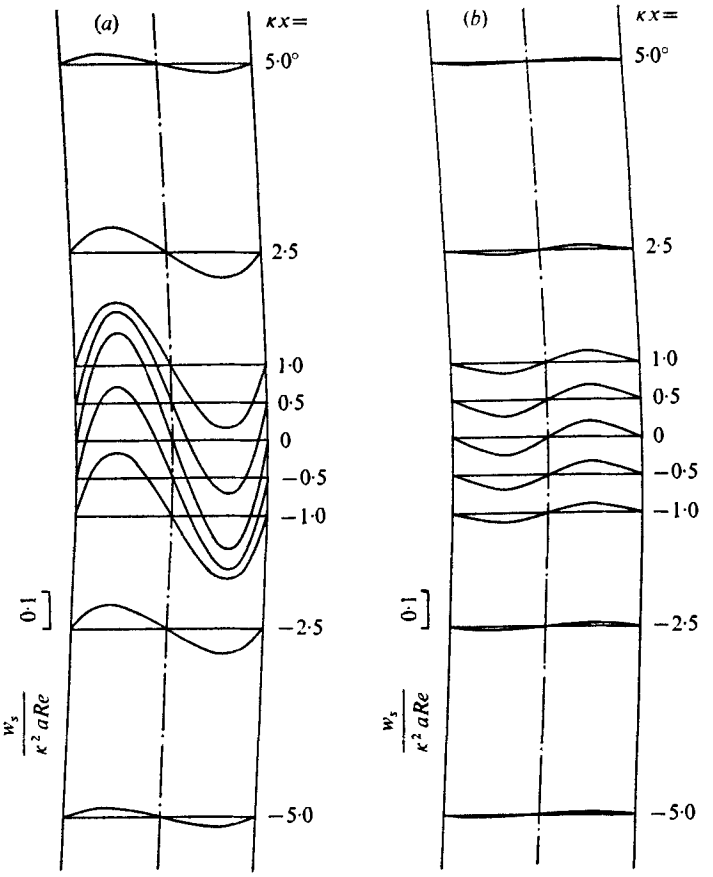

FIGURE 8. Distribution of w_s. $\kappa = 0{\cdot}01$, $\sin\phi = 0$. (*a*) $Re = 1$. (*b*) $Re = 100$.

not much different from those of figure 5(*a*) in the range computed, since the variation in centre-line curvature is vanishingly slow. In this type of pipe, the secondary flow fades out some distance from the curved region, and the flow returns to the Poiseuille regime. One may get an idea, of the axial extent of the region where secondary flow exists by considering $u_c = u/\kappa^2 aRe$, the radial velocity component of secondary flow at $r = 0$. The sections where the ratio of the absolute value $|u_c|$ at that section to its maximum $|u_c|_{\max}$ becomes 0·01 are at $\kappa x = 4{\cdot}54$ for $Re = 1$, and $\kappa x = 4{\cdot}55$ for $Re = 100$, when $\kappa = 0{\cdot}01$. In this example, secondary flow exists in a region about 450 times the pipe radius from the section of maximum curvature. This large value is partly because the variation in centre-line curvature is very small.

3.3. *Twice-curved pipe*

The flow pattern is completely analogous to that in §§ 3.1 and 3.2. Only one example, showing the axial velocity distribution, is given in figure 9. The phenomena that characterize the flow depending on the Reynolds number and κ are explained just as above. In this type of pipe, too, there appears the unusual secondary flow pattern that appeared in the periodically-curved pipe, because

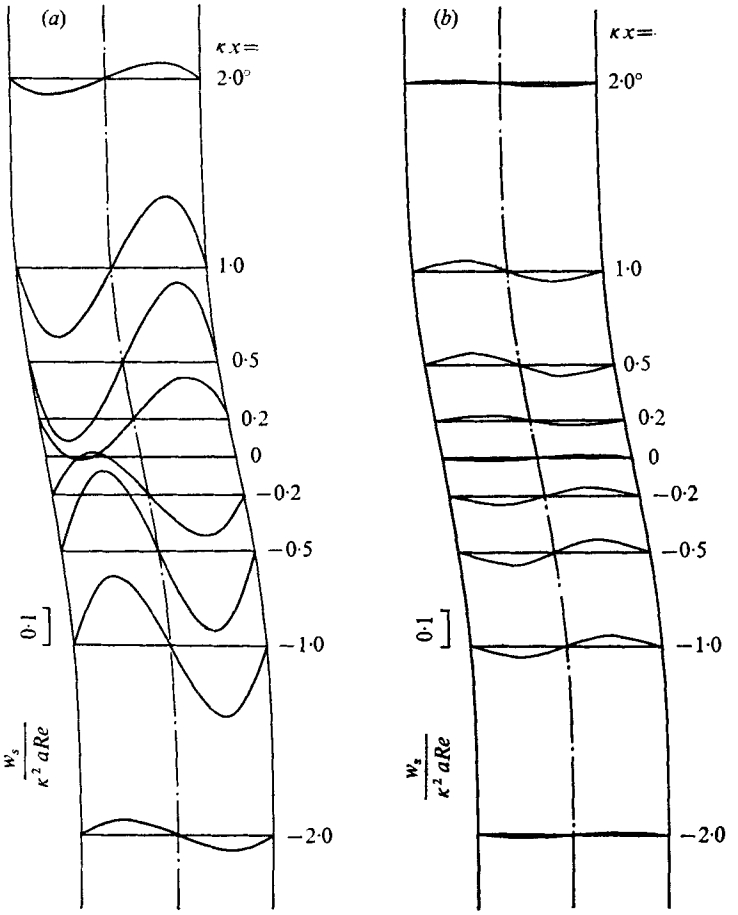

FIGURE 9. Distribution of w_s. $\kappa = 0{\cdot}1$, $\sin\phi = 0$. (*a*) $Re = 1$. (*b*) $Re = 100$.

the sense of centre-line curvature is not unique. The character of the secondary flow in that case is just as before, within the scope of this analysis, which is restricted to $\kappa \ll 1$. The sections in which the secondary flow fade out are, when the criterion of §3.2 is applied, $\kappa x = 3{\cdot}58$ for $Re = 1$ and $\kappa x = 3{\cdot}39$ for $Re = 100$ when $\kappa = 0{\cdot}01$. This means that the secondary flow exists in the region about 350 pipe radii from the inflexion point of the centre-line, and is shorter than for the once-curved pipe. The reason is that inversion of centre-line curvature produces the counter-rotating secondary flow downstream of the inflexion section.

4. Conclusions

A regular perturbation analysis of the laminar flow through pipes of circular cross-section, with the restriction that centre-line curvature is fairly small, revealed the following. At sufficiently small Reynolds number, axial flow is shifted to the inner part of a section. At high Reynolds number, on the contrary,

it is shifted to the outer region, the mechanism generating the secondary flow being fundamentally different. In the low Reynolds number range, the flow pattern is determined by the local condition, so as to make energy dissipation minimum. At high Reynolds number, the flow regime in a section reflects the history of the pipe curvature. The adaptation of flow to curvature is more and more delayed as the Reynolds number increases. The delay also increases with wavenumber, in the case of a sinusoidally-curved pipe.

The authors wish to express their thanks to Professor H. Ito of Tohoku University, Sendai, Japan, for his helpful suggestions in the course of discussion of the calculated results.

REFERENCES

ADLER, M. 1934 *Z. angew. Math. Mech.* **14**, 257.
DEAN, W. R. 1927 *Phil. Mag.* **4**, 208.
DEAN, W. R. 1928 *Phil. Mag.* **5**, 673.
GREENSPAN, D. 1973 *J. Fluid Mech.* **57**, 167.
ITO, H. 1951 *Trans. Japan Soc. Mech. Engrs.* **17**, 99.
ITO, H. 1969 *Z. angew. Math. Mech.* **49**, 653.
ITO, H. & MOTAI, T. 1974 *Rep. Inst. High Speed Mech. Tohoku Univ.* **29**, 33.
LARRAIN, J. & BONILLA, C. F. 1970 *Trans. Soc. Rheol.* **14**, 135.
LYNE, W. H. 1970 *J. Fluid Mech.* **45**, 13.
MCCONALOGUE, D. J. & SRIVASTAVA, R. S. 1968 *Proc. Roy. Soc.* A **307**, 37.